Soil Modeling for Mine Blast Simulation

Frank Marrs, Mike Heiges

Georgia Tech Research Institute, Atlanta, GA, USA

Abstract

This paper presents the results of an effort to correlate an LS-DYNA® simulation of a buried mine blast with published experimental test data. The focus of the study was on simulating the effects of soil moisture content on the blast characteristics. A mathematical model for sand is presented that is based on several previously proposed models. The simulation correlates well with the results of a mine blast experiment, thus validating the material model for sand at varying levels of saturation. The model provides an excellent baseline for blast simulations of buried mines and a soil material model that can be expanded to include higher fidelity modeling, different soil types, and real-world applications.

Introduction

Background

Over the past decade significant effort has gone into developing personnel carriers that are substantially more resistant to landmines and improvised explosive devices (IEDs). While live fire testing on these vehicles is crucial to validating their effectiveness, the tests are expensive, the test variables can be difficult to control, and the results can show significant variability, depending on which parameters are being measured. The purpose of this investigation was to demonstrate the ability of modeling and simulation – specifically LS-DYNA – to reproduce test conditions using a realistic soil model.

A literature review found a number of experimental and simulation-based studies on the factors that can affect a blast response. The experimental studies were typically conducted at the sub-scale level with small test charges (50 g to 200 g of C4 or TNT). The tests involved either a series of pressure probes mounted above the charge or a moveable plate to capture the impulse imparted by the explosion. Investigators have examined the effects of the depth of burial, soil composition, soil moisture content, location of the detonation point, charge shape, and type of explosive. Of these, soil moisture content can be a difficult test parameter to control, particularly in large scale testing. Being able to use modeling and simulation to account for soil moisture variation could significantly improve the analysis of test results.

This study focused on simulating a blast event using the high strain rate finite element analysis solver LS-DYNA and correlating the results with published test data. The soil model used explicitly reproduces the effects of the soil moisture level. This paper presents a brief description of the published experimental results used for the simulation correlation study followed by a description of the LS-DYNA simulation set up. A detailed description of the soil

modeling methods is also presented. The simulation results are then compared to the experimental data along with a discussion on the quality of the correlation.

Experiment Description

Anderson [1] conducted a series of blast experiments consisting of a buried high explosive (HE) and a momentum plate suspended above the charge. The explosive used in the experiment was 625 g of Composition B with a 10 g PET-N detonator located bottom-center of the charge. The explosive was buried with the top of the disk 5 cm beneath the surface of the sand. The disk had dimensions of 3.7 cm in height and 11.3 cm diameter, giving it a ratio of height to diameter of approximately H/D=1/3. Figure 1 depicts the experimental setup.

The momentum plate was a flat, square plate of steel measuring 80 cm x 80 cm x 6 cm and weighing 300 kg. The plate was supported by posts 20 cm above the surface of the sand for most of the experiments. In one case, the plate was positioned 30 cm above the sand. In addition to the flat steel plate, two V-shaped steel plates were also tested. One plate had a 90 degree internal angle while another plate had a 120 degree internal angle. The V-shaped plates were suspended so that the center of mass was 25 cm above the surface of the sand.

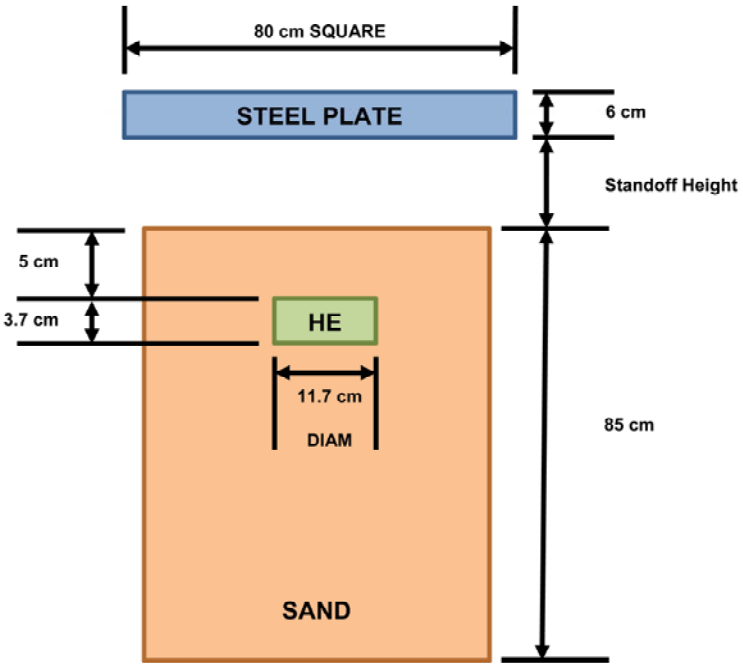

Figure 1: Dimensioned diagram of experimental setup

The sand used in the experiment was described as “common silica sand”. Grain size was less than 1 mm diameter with 99% of the sand having a grain size less than 0.5 mm. As delivered, the sand had a mass density of 1.37 g per cubic centimeter and a moisture content of 7%. Moisture percentages of 14% and 22% were also tested. The mass densities at these moisture levels were 1.49 g/cm3 and 1.67 g/cm3, respectively. The type or method of moisture content measurement is not described; however, the tolerance on the measurement is given as ±0.03 g/cm3.

The vertical displacement of the plate from its initial position was measured using cable-pull potentiometers. The maximum height was the resultant variable, which was verified using high speed video. Additionally, the accuracy of the cable-pull potentiometers was verified in one experiment using a plate-mounted accelerometer. The "jump velocity" – the theoretical maximum velocity of the plate – was calculated using

$$V_j = \sqrt{2gH}$$

where V_j is the jump velocity, H is the maximum height that the plate reaches, and g is the acceleration of gravity at sea level. Note that this equation neglects air resistance. For each experimental setup, three experiments were performed. The resulting jump velocities are given in Table 1. Generally, the results show good repeatability.

Table 1: Experimental Matrix and Jump Velocity Results

Experiment Setup	Sand Density (g/cc)	Moisture Content	Steel Plate Type	Standoff (cm)	Avg. Jump Velocity (m/s)
1	1.37	7%	Flat	20	6.60
2	1.37	7%	Flat	30	5.45
3	1.37	7%	V-Plate 90°	25	2.63
4	1.37	7%	V-Plate 120°	25	3.82
5	1.49	14%	Flat	20	7.18
6	1.67	22%	Flat	20	8.37

Mathematical Model

Air, Explosive, and Plate Models

LS-DYNA [2] was used to simulate the mine blast in three dimensions. The air, soil, and explosive were modeled as a single mesh domain of multi-material Arbitrary Langrangian Eulerian (ALE) elements measuring 60 cm square by 135 cm in height. All ALE mesh elements were cubic or very nearly so. The vertical direction of plate motion was chosen as the Y-direction. Symmetry of the model was enforced at X = 0 and Z = 0 to reduce the number of

Table 2: *MAT_NULL inputs for air (kg, m, s)

Density	Pressure Cutoff	Viscosity
1.3	-1.00E-10	2.00E-05

Table 3: *EOS_POLYNOMIAL inputs for air (kg, m, s)

C0	C1	C2	C3	C4	C5	C6	E0	V0
0	0	0	0	0.4	0.4	0	2.5e+05	1.0

elements by three quarters; this accounted for two boundary surfaces. Movement at the bottom of the soil (Y = -85 cm) was constrained in the Y direction. Non-reflecting boundary conditions

were applied to the remaining surfaces such that the air and soil were assumed to be infinite in X and Z. The air was assumed to extend infinitely in Y. The default material for all elements was specified as air, then the soil and explosive were carved out of the mesh using the *INITIAL_VOLUME_FRACTION_GEOMETRY card.

The air above the sand spanned from height Y = 0 to Y = 50 cm and was modeled as *MAT_NULL (material type 9). Standard parameters were chosen for the density of air at sea level, viscosity, and the equation of state. The parameters selected are given in Tables 2 and 3. In Table 3, C0 – C6 are the polynomial equation coefficients, E0 is the initial internal energy per unit reference specific volume, and V0 is the initial relative volume. For all LS-DYNA inputs, the LS-DYNA theory manual [2] provides more detail regarding the equations and theory behind modeling parameters.

The explosive was modeled within the ALE domain previously described. The material model, *MAT_HIGH_EXPLOSIVE_BURN, treats the products of the explosion as purely gaseous, making the choice of ALE elements appropriate. The parameters for Composition B were experimentally determined in Urtiew et. al [3]. These parameters were used to populate the material card (Material Type 8, *MAT_HIGH_EXPLOSIVE_BURN) and the equation of state card (*EOS_JWL) for the Jones, Wilkins, and Lee equation of state for an explosive [4]:

$$p = A\left(1 - \frac{\omega}{R_1 V}\right)e^{-R_1 V} + B\left(1 - \frac{\omega}{R_2 V}\right)e^{-R_2 V} + \frac{\omega E}{V}$$

Tables 4 and 5 present the values used to populate these cards.

Table 4: *MAT_HIGH_EXPLOSIVE_BURN inputs for Comp B (kg, m, s)

Density	Detonation Velocity	Chapman-Jouget Pressure	Beta (burn flag)
1700	8000	3.00E+10	2

Table 5: *EOS_JWL inputs for Comp B (kg, m, s)

A	B	R1	R2	Omega	E0	V0
5.24E+11	7.68E+09	4.2	1.1	0.50	8.50E+09	1.0

The modeling of the sand was significantly more complex than that of air and is discussed in the following section.

The steel plates were modeled using Lagrangian elements of type 2 in LS-DYNA; the average mesh size of the plate was the same as that in the ALE elements. Although the elements in the flat plates were cubic, the elements in the V-plates contained a limited number of partially skewed elements. Standard properties for steel (see Table 6) were selected for the flat plate model, although the density was altered so that the mass of the plate was exactly 300 kg. The *MAT_ELASTIC card was used to account for elastic deflections of the steel plate. Yielding of the plates was not considered. The jump velocity was assumed to be the maximum rigid body velocity in the Y-direction; this is the average of the Y-component of the nodal velocities of the plate.

The V-plates were modeled using the same material properties as the flat plate; however, the material densities were modified to match the plate masses given in Anderson. The welded-on stiffening plates from the experiment were not modeled. Instead, the stiffness of the plates was scaled to account for this omission. The V-plates with stiffening plates were modeled in Solidworks® simulation and deflected with a normal pressure of 2 MPa. Then, the stiffness of V-plate models without stiffening plates was scaled up to match the deflection of the stiffened plates. The parameters used for the 90- and 120-degree plates are given in Table 7. The height of the center of gravity for each plate was also determined. The height of the CG was 170 mm and 130 mm above the bottom edge of the V-plate for the 90-degree and 120-degree plates, respectively.

Table 6: *MAT_ELASTIC inputs for flat steel plate (kg, m, s)

Density	Young's Modulus	Poisson's Ratio
7813	4.20E+11	3.30E-01

Table 7: V-Plate Parameters

Plate	Density (g/cc)	Poisson's Ratio	Stiffness (Pa)
90°	8.682	0.33	5.0E+11
120°	8.422	0.33	4.2E+11

Table 8: Example *CONSTRAINED_LAGRANCE_IN_SOLID card

SLAVE	MASTER	SSTYP	MSTYP	NQUAD	CTYPE	DIREC	MCOUP
4	1	1	1	5	4	2	-93
START	**END**	**PFAC**	**FRIC**	**FRCMIN**	**NORM**	**NORMTYP**	**DAMP**
0.00E+00	1.00E+10	0.1	0	0.40	0	1.0	0
CQ	**HMIN**	**HMAX**	**ILEAK**	**PLEAK**	**LCIDPOR**	**NVENT**	**BLOCKAGE**
0	0	0	2	0.1	0	0	0

The interaction between the solid plate and the three fluid models – air, explosive products, and soil – bears mentioning. The fluid-structure interaction (FSI) is the key to determining the reaction of structures to explosions. LS-DYNA employs a penalty-based coupling approach. This means that each time a specified number of time steps has elapsed, the code checks for penetration of the fluids into the structure. When penetration is detected, a weighted force proportional to the penetration distance is applied. This approach is clearly non-physical. However, the current paper validates the non-physical approach as only the simplest parameters were chosen, yet good correlation was achieved. A single FSI card (*CONSTRAINED_LAGRANGE_IN_SOLID) was used to couple each fluid to the solid plate, for a total of three FSI cards – see Table 8 for an example. Since the densities and stiffnesses were very different between the materials being coupled and the speed of impact was high, the ILEAK flag was turned on (set ILEAK=2) for all FSI cards. Otherwise, all the options used in the code were the default ones. The FRCMIN flag was set to 0.4-0.6 for each coupling so that the couplings did not "turn on" at the same time. The number of quadrature points NQUAD was set to 5. All other flags defined the materials used in the coupling.

Soil Material Model

LS-DYNA offers several material models that can be used to represent soil. The soil material model selected for this analysis was *MAT_SOIL_CONCRETE (material type 78). The main components of the model are the normal stress – volumetric strain relationship and the plastic yield function. The stress-strain relationship presented here for partially saturated soil is based on the thesis by Fiserova [5] and the yield function is a modified version of that presented in Laine and Sandvik [6].

Fiserova's method for developing the stress-strain relationship for partially saturated soil is based on a relative volume approach. Soil consists of solid granular particles and inter-particle voids filled with either air or water. The density of soil, ρ, is defined by

$$\rho = \frac{m_s + m_a + m_w}{V_s + V_a + V_w}$$

where m represents mass, V is the partial volume with the subscript s denoting the solid portion of the soil, a denoting air, and w denoting water. For dry soil $V_w = 0$ and $m_w = 0$. Assuming the mass of the air is negligible, the dry density, ρ_d, can be expressed as

$$\rho_d = \frac{m_s}{V_s + V_a}$$

The initial bulk density, ρ, can be expressed in terms of the dry density and water content, ω:

$$\rho = \rho_d(1 + \omega)$$

The void ratio, e, is defined by

$$e = \frac{V_a + V_w}{V_s} = \frac{\rho_s}{\rho_d} - 1$$

where ρ_s is the average density of the solid particles. Porosity, n, is defined as

$$n = \frac{V_a + V_w}{V_s + V_a + V_w} = \frac{e}{1 + e}$$

The degree of saturation, S_r, is defined as

$$S_r = \frac{V_w}{V_a + V_w} = \frac{\omega \rho_s}{e \rho_w}$$

where ρ_w is the density of water, 1000 kg/m3.

The initial relative volumes of the air, water, and solid particles are defined as

$$\alpha_{a_0} = \frac{V_a}{V_s + V_a + V_w} = n(1 - S_r)$$

$$\alpha_{w_0} = \frac{V_w}{V_s + V_a + V_w} = nS_r$$
$$\alpha_{s_0} = \frac{V_s}{V_s + V_a + V_w} = 1 \quad n$$

The relative volumes for air, water, and solid particles under pressure are calculated using their respective equations of state. The equations of state for air and water are well established:

$$\alpha_{a_p} = \alpha_{a_0}\left(\frac{p}{p_0}\right)^{-1/k_a}$$
$$\alpha_{w_p} = \alpha_{w_0}\left(\frac{p - p_0}{\rho_{w_0} c_{w_0}^2} k_w + 1\right)^{-1/k_w}$$

where p is the pressure, k_a=1.4, k_w=3, and c_w is the speed of sound in water (1,414 m/s). The equation of state for solid particles is not known, but the relative volume for the solid particles under pressure is assumed to have the form:

$$\alpha_{s_p}/\alpha_{s_0} = a_s(p - p_0)^{k_s}$$

where a_s and k_s are unknown. These variables -- a_s and k_s -- can be solved for given pressure-strain data for soil at a specified saturation level; it is assumed that these variables are constant with respect to pressure. The density of the soil under pressure can be expressed as

$$\rho_p = \frac{\rho_0}{\alpha_{s_p} + \alpha_{a_p} + \alpha_{w_p}}$$

Table 9: Laine and Sandvik Sand Data at 6.57% Moisture Content

Parameter	Symbol	Value
Moisture content	ω	0.0657
Dry density	ρ_d	1.574E+03
Solid particle density	ρ_s	2.641E+03
Initial bulk density	ρ_0	1677
Void ratio	e	0.68
Porosity	n	0.40
Density of water	ρ_w	1000
Saturation	S_r	0.256
Initial relative air vol.	α_{a0}	0.30
Initial relative water vol.	α_{w0}	0.10
Initial soil relative vol.	α_{s0}	0.60

Using the pressure-density data provided by Laine and Sandvik and calculating the relative volumes of air and water based on their equations of state, the relative volume of the solid particles, α_{sp}, can be found as a function of pressure using the previous equation.

#

$$\alpha_{s_p} = \frac{\rho_0}{\rho_{s_p}} - \alpha_{a_p} - \alpha_{w_p}$$

Since no soil data were given in Anderson, Laine and Sandvik's data was used as the baseline test data to define the parameters a_s, and k_s for sandy soil. The sand used for these tests was relatively similar to that used in Anderson, with a moisture content of 6.57% and a "dry density" of 1.574 g/cm3. It was assumed that the "dry density" did not include the 6.57% moisture. Finally, the Laine and Sandvik sand was described as "medium to coarse" rather than the mostly medium and fine sand of Anderson. The values calculated for Laine and Sandvik sand data at 6.57% moisture content are listed in Table 9.

The relative volume of the solid particles (from Laine and Sandvik) were plotted against pressure and fitted with an exponential curve to determine a_s and k_s (Figure 2). The endpoint values are removed as possible outliers (positions of high and low compression). The values of a_s and k_s are found to be 5.9267 and -0.0926, respectively.

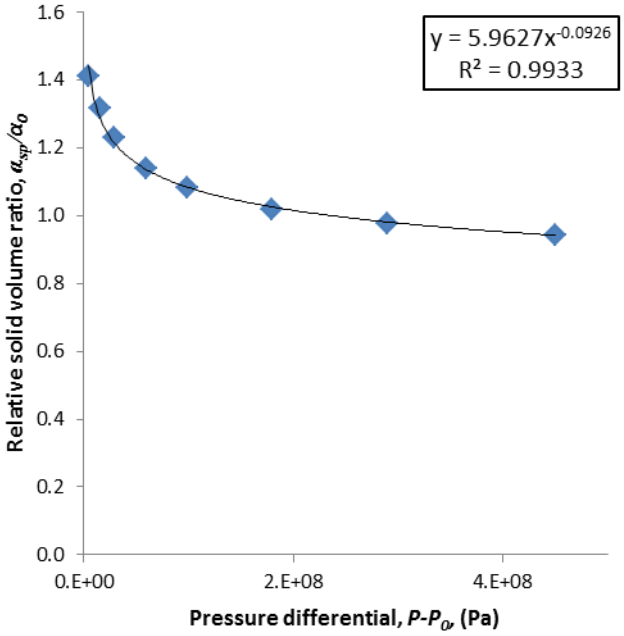

Figure 2: EOS for Soil Solid Particles Using Laine and Sandvik Data

Once a_s and k_s are known, the relative volume of the solid particles can be found for the sandy soil at any level of water content. Table 10 presents the initial density and relative volumes for the three levels of saturation used in Anderson. The particle density was assumed to be the same as in Laine and Sandvik and the dry density was adjusted to meet the water content and wet densities given in Anderson. This adjustment in dry density should account for some of the differences in particle size between the studies. The dry density varied slightly with water content; it was assumed that wet density was a more important parameter to match.

Table 10: Sand Data at Various Moisture Contents

Parameter	Symbol	7%	14%	22%
Moisture content	ω	0.07	0.14	0.22
Initial Dry Density (kg/m^3)	ρ_d	1280	1310	1390
Initial bulk density (kg/m^3)	ρ_0	1370	1490	1690
Initial relative air vol.	α_{a0}	0.43	0.32	0.17
Initial relative water vol.	α_{w0}	0.09	0.18	0.30
Initial soil relative vol.	α_{s0}	0.48	0.48	0.52

Several departures were taken from the Fiserova derivation of strength model and equation of state of the soil: the theoretical maximum density was included, cohesion was considered, Poisson's ratio was calculated, and the volumetric strain was defined as positive in compression.

First, the theoretical maximum density of the soil was enforced. As pressure increases, air is expelled from the soil. Then, compression of the soil is due to bulk modulus deflection rather than the more complex three-phase compression described above. This change in modulus of the soil was enforced.

The density at zero pressure of the theoretical maximum density can be calculated from a volume-weighted average of the densities of water and the solid soil:

$$\rho_{TMD} = \frac{\rho_{w0}\alpha_{w0} + \rho_{s0}\alpha_{s0}}{\alpha_{w0} + \alpha_{s0}}$$

Under pressure, the theoretical maximum density material was assumed to compress linearly along a line of constant bulk modulus. The bulk modulus, K_{TMD}, was defined based on the definition of the bulk modulus of mixtures [7].

$$K_{TMD} = \frac{K_w K_s}{K_w \alpha_{s0} + K_s \alpha_{w0}}$$

The bulk modulus of water is approximately 2.16E+9 Pa and the bulk modulus of the soil particles was assumed to be 5.67E+10 Pa, from Laine and Sandvik. The relationship between pressure and density can be computed from the definition of bulk modulus.

$$K = \rho \frac{\partial P}{\partial \rho}$$

$$\frac{\partial P}{\partial \rho}_{TMD} = \frac{K_{TMD}}{\rho_{TMD}}$$

Then, there is a pressure-density curve that defines the soil without air – referred to here as the line of theoretical maximum compaction – across which the pressure-density relationship of the complete soil material cannot cross.

$$P_t = \left(\frac{\partial P}{\partial \rho}_{TMD}\right)(\rho_t - \rho_{TMD})$$

This limit was imposed on the computed pressure-density relationships after computation.

Note that at very low pressure levels and high levels of saturation, the approach to developing the EOS in this study has an unrealistic artifact. The volumetric strain, ε, is initially negative; i.e., the volume initially "increases" as the pressure increases. This is caused by the assumption that all three materials (air, water, and solid particles) are always under the same pressure. When this pressure is used in the EOS for air, the calculated air density increases significantly or the volume decreases significantly. To balance out the densities of the air, water, solid particle mixture to match the soil test data, the volume of solid particles expands initially; i.e., the volume of solid particle under pressure is higher than the volume under nominal pressure. In reality, the structure of the solid particles is able to bear pressure loading so that the air voids are under a lower pressure and do not collapse as quickly. At much higher pressures the soil acts like a fluid and all three components are under the same pressure. Because explosions occur at very high pressures, the low pressure expansion artifact does not appear to adversely affect the simulation results. Interpolation data points were chosen so that this mathematical anomaly was avoided.

The computation of EOS for the various densities went as follows. First, ten pressure data points were selected. The constitutive equations for volume fraction were imposed to find the relative volume fractions of soil, air, and water at each of the ten pressures. Then, the density was calculated at each of the ten pressure values. Each point was checked to ensure that it was to the left of the line of theoretical maximum compaction. If any density was above the theoretical maximum, the pressure-density relationship was adjusted so that the curve was parallel to the line of theoretical maximum compaction. The volumetric strains were then calculated at each of the ten pressures (defined as positive for LS-DYNA).

$$\varepsilon_t = -ln\left(\frac{\rho_0}{\rho_t}\right)$$

The ten pressures were reselected so that no negative volumetric strains occurred and exactly one segment was as close as possible to the line of theoretical maximum compaction. The pressures were also chosen such that they were geometrically spaced in volumetric strain. These ten pairings of (gage) pressure and volumetric strain defined the EOS for the sand at three separate levels of water content. The plots of these EOS, along with Laine and Sandvik data, are presented in Figure 3.

The strength model was the same as that in Fiserova, a Mohr-Coulomb model of failure. In this model, the yield stress is linear in pressure,

$$Y = c + P\tan(\phi)$$

where c is the maximum tension the soil can carry (cohesion), P is the applied pressure, and ϕ is the friction angle. In Fiserova, it is assumed that the friction angle is a constant and the Poisson's ratio, ν, is calculated. However, in the current paper, it is assumed that the Poisson's ratio varies with water content (as a volume-weighted average). Using the partial volume approach

$$\nu = \nu_s \alpha_{s_0} + \nu_w \alpha_{w_0} + \nu_a \alpha_{a_0}$$

where ν_w=0.4999 and ν_a=0.0001. Poisson's ratio for the solid particles, ν_s, is found to be 0.222, again using Laine and Sandvik's data as a reference. The friction angle is calculated from the Poisson's ratio,

$$\phi = \sin^{-1}\frac{2\nu - 1}{\nu - 1}$$

#

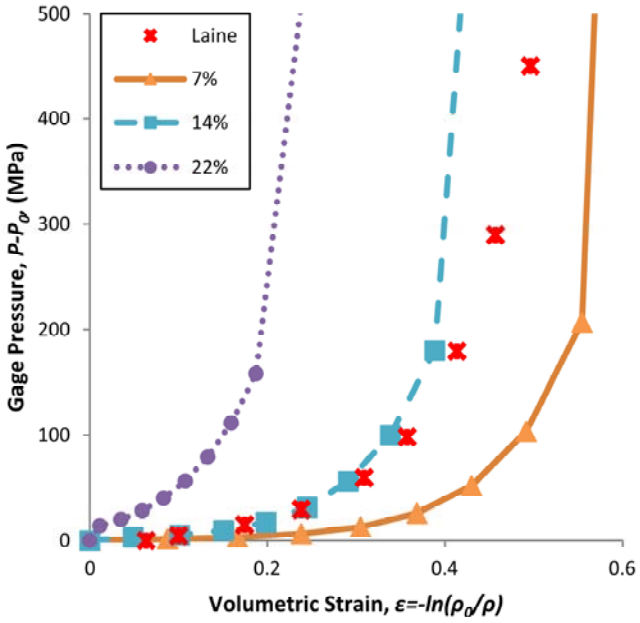

Figure 3: EOS models of sand for varying water contents

The value of the friction angle was assumed to be constant throughout the range of pressures (although it does vary with water content). Although the Poisson's ratio varies during compression, the changes in friction angle are very small with respect to changes in Poisson's ratio based on the equation above.

Cohesion, c, was calculated from Grujicic et. al. [8],

$$c = w^5(729\,\text{kPa})$$

where w is the water content. This parameter was expected to make little difference in results but was included for completeness, as sandy soil does not adhere to itself much.

The yield stress was linear up to an assumed maximum of 2.26E6 Pa, the unconfined strength of Pike's Peak Granite and an estimated maximum of the soil particles, as in Laine and Sandvik. The strength curves are presented in Figure 4.

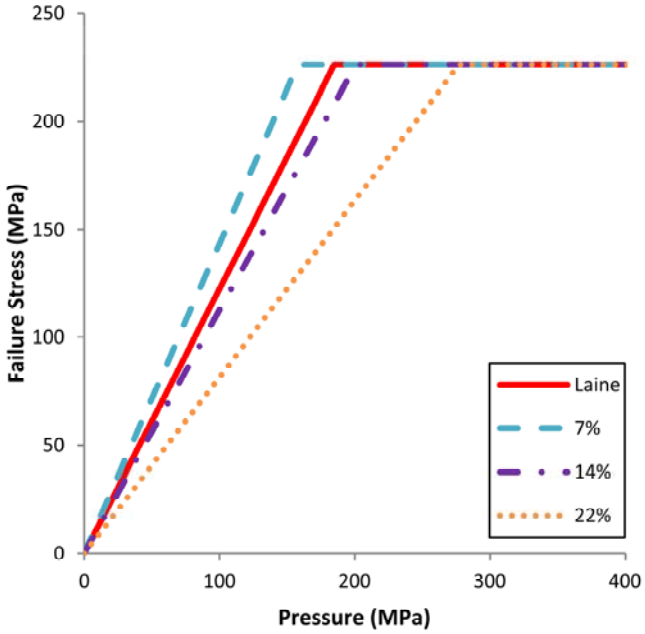

Figure 4: Strength models for varying water contents of sand

The bulk modulus, K, was calculated as a function of pressure and density from the definition of bulk modulus,

$$K_t = \rho_t \frac{P_t - P_{t-1}}{\rho_t - \rho_{t-1}}$$

and the shear modulus, G, was calculated as a combination of Poisson's ratio and bulk modulus,

$$G = \frac{3K(1-2\nu)}{2(1+\nu)}$$

Table 11: Soil constants used in LS-DYNA simulation

	7% Moisture	14% Moisture	22% Moisture
G (Pa)	1.68E+07	3.90E+07	2.22E+08
K (Pa)	2.12E+07	4.67E+07	2.45E+08
ν	0.15	0.2	0.27
ϕ (deg.)	55.09	48.39	39.22

The material model in LS-DYNA allows only constant values for the bulk and shear moduli; i.e., the variation with pressure is not modeled. The values of K and G were selected as the values that occur at an approximate soil density of 1.6-1.7 g/cm^3. The calculated parameters for all soil types are presented in Table 11.

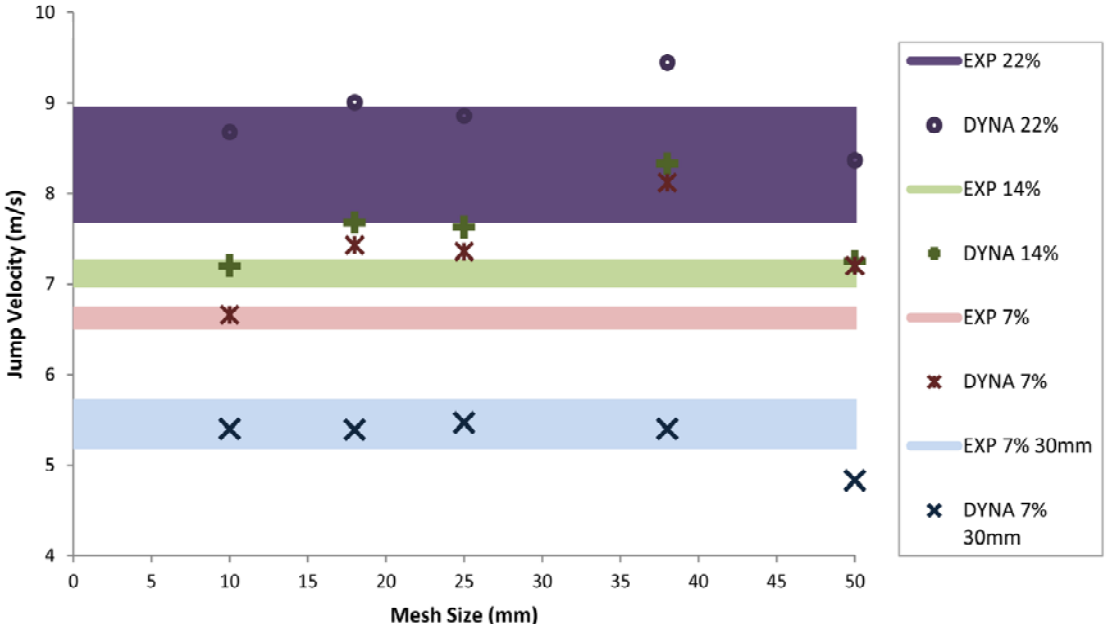

Figure 5: Flat plate simulation results

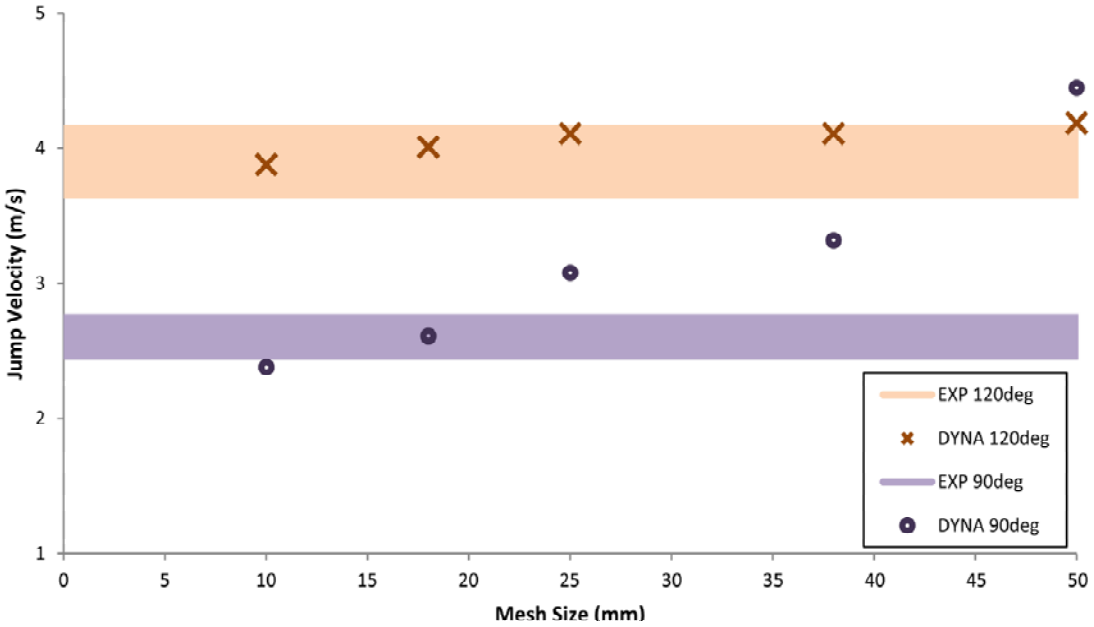

Figure 6: V- plate simulation results

Results and Discussion

In the experiment by Anderson the "jump velocity" was used to evaluate the resulting energy of explosion delivered to the steel momentum plates. The LS-DYNA experiment showed excellent correlation with the experimental results. Figures 5 and 6 show the results for various mesh sizes for the flat plate and V-plate experiments, respectively. The solid bars in these figures represent the range of the experimental results.

All results show convergence as the mesh size decreases. It appears that the smallest mesh size – 10 mm – provides the best agreement, as expected. However, an 18 mm mesh

provides results that are reasonably similar to the 10 mm mesh. The flat plate results suggest that the 50 mm mesh is too coarse to characterize the blast. Note that the explosive was only 37 mm in height and 117 mm in diameter. So, the 10 mm mesh has approximately six elements in the radial direction and four elements in the thickness direction of the explosive. This is on the lower end of the recommended number of desired elements and explains why complete convergence is not observed. However, computational time was a limiting factor. A 5 mm mesh simulation would have taken several days to perform while running 30 parallel processes at 2.7 GHz processor speed each.

Table 12: Tabulated simulation results compared to experimental results

Soil Density (%)	Standoff (cm)	Plate Configuration	Average Exp. V_J (m/s)	Maximum Change V_J (m/s)	Simulation V_J (m/s)	% Error
7	20	Flat	6.60	0.15	6.66	1.0
14	20	Flat	7.18	0.17	7.20	0.3
22	20	Flat	8.37	0.79	8.68	3.7
7	30	Flat	5.45	0.31	5.40	-1.0
7	25	V-90deg	2.63	0.17	2.38	-9.6
7	25	V-120deg	3.82	0.33	3.88	1.7

The results are tabulated in Table 12. One can see the excellent agreement between the simulation and the experiment. The error is less than 10% at all points, and less than 5% in most cases. In all but one case, the simulation result falls within the variation of the experimental data. Note that the equation for the jump velocity used in Anderson neglects the air drag and gravity losses during the motion of the plate after impact. These phenomena are integrated into the LS-DYNA simulation, although their contributions are expected to be negligible. The good agreement of the simulation and experiment confirms this assumption.

The experimental data suggests a linear relationship between the soil moisture content and momentum (or jump velocity) of the flat plates at 20 mm standoff,

$$V_t = \frac{\rho_t}{\rho_0} V_0$$

Figure 7 shows the experimental results compared to those found in the LS-DYNA simulation. The simulation closely mimics the trend found in Anderson, suggesting that the density of the soil is a key parameter in momentum transfer from the blast to the structure. A linear trend line is also provided. The coefficient of determination is about 0.986, suggesting that momentum transfer may be linear in soil density.

Conclusion

The results from the LS-DYNA simulation correlate very well with the data from a mine blast experiment. These results validate an explicit material model for sand that accounts for variation in soil saturation levels. The model provides an excellent baseline for blast simulations of buried mines and a soil material model that can be expanded to include higher fidelity modeling decision, different soil types, and real-world applications.

The success of the LS-DYNA simulation opens several areas of further research. Most obviously, the model can be used to simulate the impact of real-world blasts on structures designed to survive blasts (such as military vehicles). The soil model can be extended to examine other types of soils, such as silty or clayey soils. The model can also be used to generalize the blast momentum transferred based on charge depth of burial, charge size, and soil type.

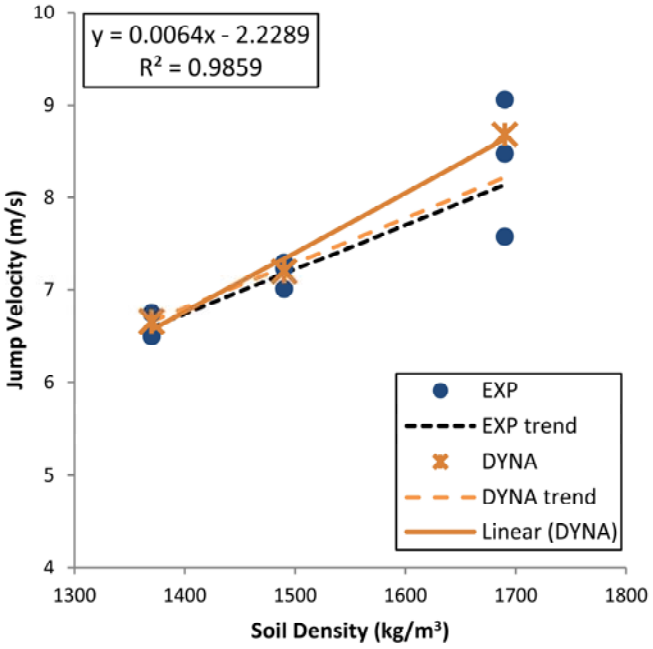

Figure 7: Variation of jump velocity with soil density

Acknowledgements

This research effort was funded by the Navy Surface Warfare Center Indian Head Division.

References

1. Anderson, C.E., Behner, T., and Weiss, C.E., "Mine blast loading experiments," International Journal of Impact Engineering, 38(8-9): 697–706 (2011)

2. Livermore Software Technology Corporation, "LS-DYNA Theory Manual," March 2006. Available online: http://www.dynasupport.com/manuals/additional/ls-dyna-theory-manual-2005-beta/at_download/file

3. Urtiew, P.A., Vandersall, K.S., Tarver, C.M., Garcia, F., and Forbes, J.W., "Shock Initiation of Composition B and C-4 Explosives; Experiments and Modeling," International Conference on Shock Waves in Condensed Matter, Saint Petersburg, Russia, September 18, 2006

4. Lee, E., Finger, M., Collins, W., "JWL Equation of State Coefficients for High Explosives", Lawrence Livermore Laboratory, Rept-UCID-16189, (1973)

5. Fiserova, D., Numerical Analyses of Buried Mine Explosions with Emphasis on Effect of Soil Properties on Loading, PhD thesis, Defence College of Management and Technology, Cranfield University, Jan. 2006

6. Laine, L and Sandvik, A., "Derivation of Mechanical Properties for Sand," Proceedings of the 4th Asia-Pacific Conference on Shock and Impact Loads on Structures, CI-Premier PTE LTD, 361-368, Singapore, Nov. 2001,

7. Bar-Meir, Genick, Basics of Fluid Mechanics, pg. 29, Chicago, IL, 5 December 2010

8. Grujicic, M., Pandurangan, B., Qiao, R., Cheeseman, B., Roy, W., Skaggs, R., and Gupta, R., "Parameterization of the Porous-Material Model for Sand with Different Levels of Water Saturation," Soil Dynamics and Earthquake Engineering, Vol. 28: 20-35, 2008